Evolution of a Rippled Membrane during Phospholipase A_2 Hydrolysis Studied by Time-Resolved AFM

Chad Leidy,*† Ole G. Mouritsen,*§ Kent Jørgensen,*‡ and Günther H. Peters*†
*MEMPHYS-Center for Biomembrane Physics, †Department of Chemistry, and ‡LiPlasome Pharma A/S, Technical University of Denmark, DK-2800 Lyngby, Denmark; and §Department of Physics, University of Southern Denmark, DK-5230 Odense M, Denmark

ABSTRACT The sensitivity of phospholipase A_2 (PLA_2) for lipid membrane curvature is explored by monitoring, through time-resolved atomic force microscopy, the hydrolysis of supported double bilayers in the ripple phase. The ripple phase presents a corrugated morphology. PLA_2 is shown to have higher activity toward the ripple phase compared to the gel phase in 1,2-dimyristoyl-*sn*-glycero-3-phosphocholine (DMPC) membranes, indicating its preference for this highly curved membrane morphology. Hydrolysis of the stable and metastable ripple structures is monitored for equimolar DMPC/1,2-distearoyl-*sn*-glycero-3-phosphocholine (DSPC)-supported double bilayers. As shown by high-performance liquid chromatography results, DSPC is resistant to hydrolysis at this temperature, resulting in a more gradual hydrolysis of the surface that leads to a change in membrane morphology without loss of membrane integrity. This is reflected in an increase in ripple spacing, followed by a sudden flattening of the lipid membrane during hydrolysis. Hydrolysis of the ripple phase results in anisotropic holes running parallel to the ripples, suggesting that the ripple phase has strip regions of higher sensitivity to enzymatic attack. Bulk high-performance liquid chromatography measurements indicate that PLA_2 preferentially hydrolyzes DMPC in the DMPC/DSPC ripples. We suggest that this leads to the formation of a flat gel-phase lipid membrane due to enrichment in DSPC. The results point to the ability of PLA_2 for inducing a compositional phase transition in multicomponent membranes through preferential hydrolysis while preserving membrane integrity.

INTRODUCTION

Secretory phospholipase A_2 (PLA_2) catalyzes the hydrolysis of the ester linkage in the *sn*-2 position of glycerophospholipids, yielding free fatty acid and lysophospholipid (Six and Dennis, 2000). PLA_2 is interfacially activated, showing higher activity toward lipids that are aggregated, for example into a bilayer lipid membrane structure, than toward lipids that are free in solution (Verger et al., 1973; Waite, 1991). PLA_2 plays a prominent role in physiological processes involving lipid membrane modification and generation of bioactive lipids through hydrolysis. These processes include pro-inflammatory response (Nevalainen et al., 2000), neuronal lipid membrane repair and regeneration (Geddis and Rehder, 2003), and generation of the stratum corneum (Mao-Qiang et al., 1995). PLA_2 has been suggested to be involved in these and other processes both as a generator of signaling lipids (Murakami and Kudo, 2002), and as a direct modifier of lipid membrane morphology (Brown et al., 2003). In either case, in order for PLA_2 to induce the appropriate changes in the lipid membrane without compromising lipid membrane integrity, the enzyme activity needs to be regulated.

Several years of extensive work have shown that the physical properties of the lipid membrane play a major role in modulating PLA_2 activity (Kensil and Dennis, 1979; Dennis et al., 1981; Burack and Biltonen, 1994; Hønger et al., 1996; Høyrup et al., 2002). Structural defects and fluctuations that occur near phase transition temperatures are known to increase PLA_2 activity (Hønger et al., 1996). These perturbations in the lipid membrane structure are believed to induce packing defects that facilitate access of the enzyme to the cleavage site at the *sn*-2 position. Additionally, in giant unilamellar vesicles showing gel/fluid coexistence, PLA_2 was shown to preferentially bind and hydrolyze the fluid-phase domains (Sanchez et al., 2002).

Curvature also has a strong influence on PLA_2 activity. In the case of small unilamellar vesicles the enzyme shows sensitivity to different degrees of curvature (Bell and Biltonen, 1989). Furthermore, the enzyme has also been postulated to present increased sensitivity toward regions of high curvature achieved by product accumulation and phase separation (Burack and Biltonen, 1994; Burack et al., 1997b). Large unilamellar vesicles show under certain conditions a so-called lag-burst behavior where a long lag time of low activity is followed by a period of rapid hydrolysis (Apitz-Castro et al., 1982; Hønger et al., 1996; Nielsen et al., 1999). After this onset, the hydrolysis then occurs in a very rapid manner. The fast hydrolysis after the lag time has been attributed to product accumulation, thereby increasing the interfacial disorder that results in increased access for the enzyme to the cleavage site (Burack et al., 1993). This lag phase before hydrolysis, can be reduced with the exogenous addition of fatty acids and lysophospholipids (Burack and Biltonen, 1994). The fatty acids when ionized can contribute to increased affinity of PLA_2 to the lipid membrane surface

Submitted October 17, 2003, and accepted for publication March 31, 2004.

Address reprint requests to Chad Leidy, MEMPHYS-Center for Biomembrane Physics, Technical University of Denmark, Dept. of Chemistry, Bldg. 206, DK-2800 Lyngby, Denmark. Tel.: 45-4525-2431; Fax: 45-4588-3136; E-mail: cleidy@kemi.dtu.dk.

0006-3495/04/07/408/11 $2.00

doi: 10.1529/biophysj.103.036103

by electrostatic attraction of the positively charged enzyme. Negative charge is known to increase the affinity of PLA_2 toward the membrane. However, the fatty acids produced are not necessarily fully ionized, and it is not clear how much they contribute to increasing the activity of the enzyme (Peters et al., 2000). Lysophospholipids, on the other hand, are known to induce positive lipid membrane curvature, which increases the affinity of PLA_2 for the lipid membrane (Henshaw et al., 1998). Vesicles were observed to undergo sharp changes in morphology due to product accumulation, and these changes in morphology were correlated with an increase in PLA_2 activity (Burack et al., 1997a). These results suggest that lipid membrane curvature can be an important regulator for PLA_2 activity.

In this article we explore the sensitivity of PLA_2 toward curved bilayers by studying the activity of PLA_2 toward the ripple phase. The two most studied and well-characterized lipid phases are the gel phase and the fluid phase. Both of these lipid phases correspond to locally flat lipid membrane morphologies. The ripple phase, in contrast, has an intriguing surface morphology, characterized by corrugations in the lipid bilayer with a well-defined periodicity (Nagle and Tristram-Nagle, 2000). The origin of the ripple structure is still under investigation. Different models have been presented, attempting to explain the local spontaneous curvature observed in the ripple phase, including an electrostatic coupling between water molecules and the polar lipid headgroups (Doniach, 1979), a coupling between lipid membrane curvature and molecular tilt (Lubensky and Mackintosh, 1993), as well as the generation of curvature by linear arrays of fluid-state lipid molecules (Heimburg, 2000). Two different ripple structures can form depending on the history of the sample (Zasadzinski et al., 1988, Tenchov et al., 1989; Koynova et al., 1996; Katsaras et al., 2000). One is a stable ripple phase ($\Lambda/2$-ripples) with repeat distance around 130–150 Å, and the other is a metastable ripple phase (Λ-ripples) with repeat distance of 260–300Å which is approximately double the spacing as the stable ripple phase. The proportion of each phase depends on the thermal history of the sample, and there is a slow conversion from the metastable to the stable ripple phase. We have previously shown that the ripple phase can be visualized by atomic force microscopy (AFM) in supported double bilayers composed of 1,2-dimyristoyl-*sn*-glycero-3-phosphocholine (DMPC), 1,2-dipalmitoyl-*sn*-glycero-3-phosphocholine (DPPC) and DMPC/1,2-distearoyl-*sn*-glycero-3-phosphocholine (DSPC) mixtures, showing coexisting ripple structures (Λ- and $\Lambda/2$ ripples), ripple/fluid phase coexistence, and ripple/gel phase coexistence (Leidy et al., 2002; Kaasgaard et al., 2003). These results have shown that changes in the ripple structure can be carefully monitored by AFM in a time- and temperature-dependent manner.

The ripple phase presents an interesting model for studying lipid membrane curvature effects on PLA_2 activity, and it provides the opportunity to visualize directly by AFM the enzymatic hydrolysis of a lipid membrane surface that presents a high degree of local curvature. In the first part of the study a comparison is done between the hydrolysis of the ripple-phase DMPC bilayers compared to the gel-phase DMPC bilayers, testing the expected higher sensitivity of a ripple-phase bilayer toward hydrolysis, due to the preference of PLA_2 for curved lipid membranes. In the second part we monitor the hydrolysis of different ripple structures in 1:1 DMPC/DSPC supported double bilayers. The presence of DSPC reduces the rate of hydrolysis, making it possible to monitor in a time-dependent manner the changes in lipid membrane morphology due to both accumulation of products and variation in composition during hydrolysis. The final part of the study addresses evidence showing that hydrolysis of PLA_2 occurs preferentially along the direction of the ripples.

MATERIALS AND METHODS

DMPC, DPPC, and DSPC were purchased from Avanti Polar Lipids (Alabaster, AL) and were used without further purification. Snake venom PLA_2 (*Agkistrodon piscivorus piscivorus*) was a gift from Prof. R. L. Biltonen, University of Virginia. Ruby muscovite mica was obtained from Plano W. Plannet GmbH (Wetzlar, Germany). Appropriate amounts of DSPC and DMPC were dissolved and mixed in chloroform. The samples were then dried under nitrogen gas and placed under vacuum overnight to remove the residual solvent. The dried lipids were dispersed in Milli-Q water to a final concentration of 3 mM. In the one-component DMPC and DPPC samples the lipids were dispersed directly in Milli-Q water to a concentration of 3 mM. Aqueous multilamellar lipid dispersions were prepared by heating the samples to 65°C, followed by vortexing. Small unilamellar vesicles (SUVs) were prepared by sonication using a Labsonic U tip sonicator (B. Braun Biotech International, Melsungen, Germany) at 65°C for two periods of 7 min. Residual titanium was removed from the vesicle solution by centrifugation for 5 min at 2750 $\times$ G. The SUVs were immediately rewarmed to 65°C, and 1 ml was added to a small homebuilt cell for the atomic force microscope containing a piece of freshly cleaved mica. We find that the state of the vesicles before addition onto the mica during the incubation step is crucial. After sonication, and just before adding the vesicles onto the mica, the vesicle solution needs to be clear, which ensures that the solution consists mostly of small unilamellar vesicles. In addition, the SUV solution needs to be prepared at a high temperature, and then allowed to cool on the mica. The samples were incubated for 1 h at 24°C in the case of the DMPC-DSPC mixtures, at 17°C in the case of the DMPC samples, and at 38°C in the case of the DPPC samples. The samples were then rinsed by exchanging ten times the incubation solution with 20 mM NaCl solution and 20 μM $CaCl_2$ (required for PLA_2 activity), never allowing the supported bilayer to dry. Adding the warmed SUV solution and allowing the sample to cool down during incubation to a temperature below the solidus phase line transition was generally a successful procedure for obtaining double bilayers. The formation of double bilayers has been previously corroborated by scratching a hole down to the mica substrate at a high force setting (Leidy et al., 2002).

Atomic force microscopy

The mica supported lipid bilayers were imaged in contact mode using a PicoSPM atomic force microscope (Molecular Imaging, Phoenix, AZ). The cantilevers were oxide-sharpened silicon nitride cantilevers (Thermo-Microscopes, Sunnyvale, CA) with nominal spring constants of 0.01 N/m.

To ensure that the force was kept minimal during scanning, the force was frequently decreased until the tip left the surface and subsequently slightly increased until just regaining contact. In general, ripples could only be resolved when the force was at an absolute minimum. Due to scanner hysteresis and small variations in temperature during scanning, precise statements about the scanning force are difficult to make. Even temperature fluctuations of the order of 10^{-2}°C cause noticeable thermal bending of the gold-coated cantilevers. However, a conservative estimate of the force range would be 20–300 pN based on the nominal spring constant. PLA_2 was added to give a total concentration of ~420 nM. The total lipid concentration of the solid supported lipid bilayer system in the AFM fluid cell was ~2 μM. The protein to lipid ratio is then ~1:5.

Fluorescence spectroscopy

PLA_2 hydrolysis was studied in bulk by monitoring the release of a water-soluble fluorescent dye, calcein, encapsulated in DMPC large unilamellar vesicles (200 nm) in a self-quenching concentration (50 mM). Calcein was dissolved in water and pH adjusted with NaOH to pH = 7.5 before adding the calcein solution to the 10 mM HEPES buffer (10 mM HEPES, 1 mM KCl, 1 mM NaN_3, 30 μM $CaCl_2$, 10 μM NaEDTA). The lipid suspension was hydrated in the calcein solution as described above. The multilamellar vesicles were extruded 10 times through two stacked 200 nm pore size polycarbonate filters (Whatman, Clifton, NJ) forming large unilamellar vesicles (LUVs) with a narrow size distribution. Untrapped calcein was removed from the liposome suspension by gel filtration through a column packed with Sephadex G-50 using the HEPES buffer as eluent. Fluorescence measurements were performed using a SLM DMX 1100 spectrofluorometer. Excitation and emission channels were set at 490 nm and 515 nm respectively, and fluorescence was measured as a function of time. PLA_2 was added after 100 s and the emission fluorescence is recorded after 1000 s. 100% release is obtained by adding 50 μl of 10% Triton X-100. Plots are corrected for passive release of the calcein. The total lipid concentration for each sample was 150 μM and the enzyme concentration used was 150 nM.

Differential scanning calorimetry

DSC was performed using a MicroCal MC-2 (Northhampton, MA) on samples of 50 mM DMPC LUVs at a scan rate of 10°C/ h. An appropriate baseline was substracted from the resulting thermograms.

High-performance liquid chromatography (HPLC)

HPLC quantification of the hydrolysis reaction (Høyrup et al., 2001a) was made using a Waters Millennium 2010 system (Milford, MA) equipped with a Waters 510 pump, a Waters 717 Plus autosampler, and a PL-EMD 950 evaporative light scattering mass detector from Polymer Laboratories (Cheshire, UK) using 5 μm Phenomenex (Torrance, CA) diol spherical column and a mixture of chloroform/methanol/water (73:23:3 v/v) as isocratic mobile phase. 100 μl lipid suspension samples were retrieved directly from the reaction chamber in the fluorometer several times during the PLA_2 lipid hydrolysis time course. The extracted lipids were rapidly mixed in chloroform/methanol/acetic acid/water (2:4:1:1) to quench the PLA_2 lipid hydrolysis effectively. After quenching the PLA_2 activity it was confirmed that the composition of the sample did not change by storage. Salts were extracted from the sample by shaking thoroughly with 1 ml water. From the organic phase 20 μl was analyzed by HPLC. The degree of hydrolysis was measured by the reduction in the substrate fraction. Dose/response calibration curves were linear in the used concentration range.

RESULTS AND DISCUSSION

PLA_2 hydrolysis of a one-component DMPC supported bilayer: differences in susceptibility to hydrolysis between gel phase and ripple phase

We first explore the hydrolysis of a one component supported double bilayer in the ripple phase. Fig. 1 *a* shows a region of Λ-ripples forming in a DMPC supported double bilayer at 17°C. The average ripple spacing is found by Fourier transform to be 312 ± 4 Å. Fig. 1 *b* shows an image of the same region after addition of PLA_2. The scan is taken from bottom to top, and shows a sudden degradation of the

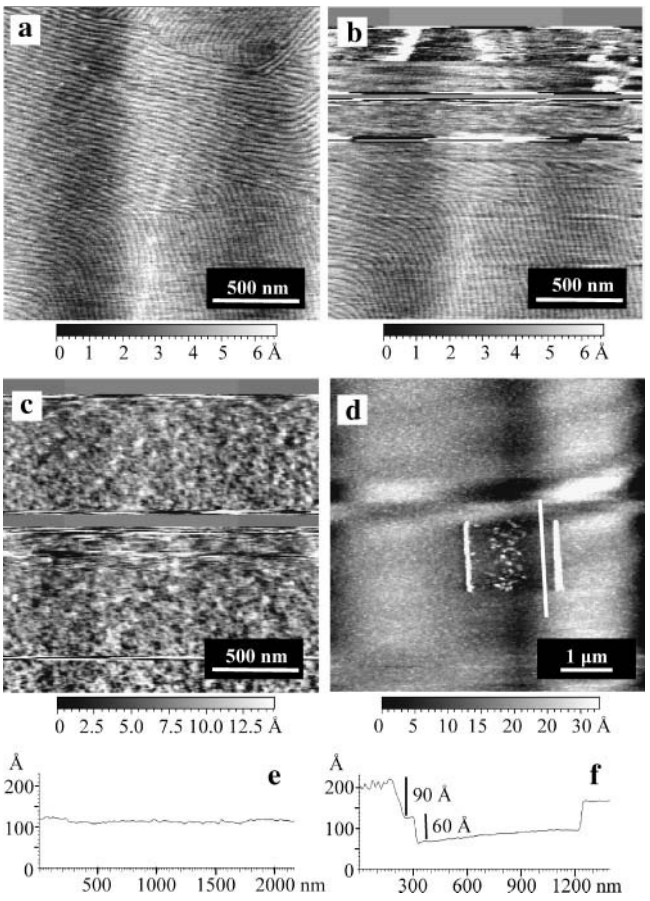

FIGURE 1 Height mode AFM images showing the stable (Λ spacing) ripple phase in DMPC supported double bilayers (*a*) before; (*b*) 5 min; and (*c*) 9 min after addition of PLA_2; (*d*) A hole is scratched on the surface using a high force setting 30 min after addition of PLA_2. The hole is delimited by two light colored stripes formed by material accumulation during scratching; (*e*) height profile is taken across the hole shown in Fig. 1 *d*. The height profile of the hole is much smaller than the expected bilayer thickness, which shows that the bilayer integrity has been lost during hydrolysis; (*f*) For comparison, the height profile of a DPPC double bilayer is presented, showing three levels corresponding to the second bilayer, first bilayer and mica. The mica has been exposed by scratching a hole at a high force setting. The height of the second bilayer is 90 Å, and the height of the first bilayer is 60 Å. All images are taken at 17°C. The height profile in *f* was taken at 38°C corresponding to the ripple temperature regime for DPPC.

lipid membrane as the scanning probe reaches the top one-third of the image. The initial stages of degradation are observed to occur within 5 min after the addition of PLA_2. Fig. 1 *c* shows the same region 9 min after addition of PLA_2. The image shows that the ripples have disappeared and the surface has become inhomogeneous, likely due to degradation of the lipid followed by incorporation of fatty acids and lysophospholipids. In Fig. 1 *d*, a hole is scratched down to the mica surface at a high force setting to corroborate that the lipid membrane has been degraded. The height profile of the hole in Fig. 1 *e* shows that the height difference between the surface features and the mica is ~10 Å, which is much smaller than the expected height for a supported bilayer. For comparison, a control showing the height profile of a DPPC supported double bilayer is presented. Fig. 1 *f* shows a height profile of a hole that has been scratched on a DPPC double bilayer down to the mica surface. The 90 Å and 60 Å bars correspond to the height profiles of the second and first bilayers respectively. From this it is clear that the 10 Å height difference observed in Fig. 1 *e* does not correspond to a bilayer. The fact that the surface is not completely cleared during hydrolysis suggests that at least part of the lipids remain attached to the mica, forming rearranged structures. The remaining features on the surface most likely correspond to aggregates of hydrolysis byproducts (i.e., fatty acids, lysophospholipids), and some remaining DMPC. Fig. 1 *d* also indicates that the bottom bilayer is not present, indicating that the bottom bilayer in the double bilayer system has been degraded along with the top bilayer. In general, the remaining aggregate does not show a defined bilayer structure.

The hydrolysis of a single supported gel-phase bilayer presenting a flat morphology evolves differently than the hydrolysis of the rippled membrane. Fig. 2 *a* shows a supported single DMPC bilayer at 17°C. The behavior of a single DMPC bilayer is significantly different than a double bilayer. Interactions of the lipid membrane with the mica surface suppress ripple formation in the single supported bilayer (Fragneto et al., 2001; Giocondi et al., 2001; Leidy et al., 2002). The lipid membrane therefore maintains a flat morphology characteristic of a gel-phase lipid membrane. The undulations seen in the image are due to noise from the temperature control stage. After addition of PLA_2, a much longer time is necessary for the lipid membrane to show signs of degradation. The first evidence of degradation is the formation of a significant number of small protrusions distributed on the surface, with a diameter of 20–40 nm (Fig. 2 *b*, 65 min), followed by the formation of holes (Fig. 2 *c*, 122 min) that grow continuously until the lipid membrane is fully degraded. Protrusions are first detected typically 1 h after addition of PLA_2, which is significantly longer than the time it takes (5 min) for degradation of the ripple-phase lipid membrane. This long lag time before initial degradation by PLA_2 is most likely related to the lag-phase studied intensively both in bulk measurements using liposomes (Apitz-Castro et al., 1982; Hønger et al., 1996; Nielsen et al., 1999) and in supported gel-phase bilayers (Nielsen et al., 1999). The duration of the lag phase in bulk measurements has been correlated with the presence of defects on the bilayer (among other factors such as composition and calcium concentration) (Fernandez et al., 1991; Hønger et al., 1996, 1998). These defects are proposed to provide the enzyme with easier access to the carbonyl backbone of the phospholipid for hydrolysis. Other AFM studies have shown that in the presence of preformed holes no lag phase is observed (Grandbois et al., 1998; Kaasgaard et al., 2001). In these cases, hydrolysis is shown to take place at the hole edges where the surface curvature is high, providing an exposed site for hydrolysis. The formation of protrusions in Fig. 2 *b*, which seem too large (20–40 nm) to correspond to individual proteins, which have a diameter of ~4 nm (Han et al., 1997), are most likely a result of product accumulation, serving as sites for hydrolysis to progress, leading to formation and growth of holes.

The long lag period observed in Fig. 2 may then be understood in terms of a reduced number of defects in the supported bilayer. Bilayers formed by vesicle fusion exhibit less number of holes than lipid membranes formed by Langmuir-Blodgett deposition (Kaasgaard et al., 2001; Leidy et al., 2002). Probing of the DMPC-supported bilayer deposited through vesicle fusion (Fig. 2 *a*) shows no evidence of holes, which appears to indicate close to complete coverage of the mica. The lack of evident defects is therefore most likely the cause for the delay in the initiation of hydrolysis. On the other hand, when DMPC is in the ripple phase, hydrolysis begins almost immediately after

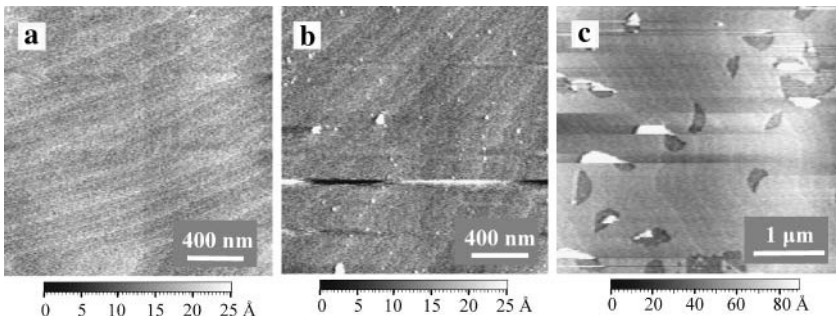

FIGURE 2 Height mode AFM images showing a single supported DMPC bilayer (*a*) before, (*b*) 65 min, and (*c*) 122 min after addition of PLA_2. The protrusions on the lipid membrane surface observed in *b* are the first indication of hydrolysis of the lipid membrane. This is followed by formation and growth of holes as seen in *c*.

addition of PLA_2. The very fast kinetics of hydrolysis observed for DMPC supported double bilayers in the ripple phase, even in the absence of any apparent defects in the lipid membrane (Fig. 1), indicate that the undulated surface provides PLA_2 with easier access to the substrate.

These observations are also supported by bulk hydrolysis measurements. Fig. 3 *a* shows fluorescence measurements done on large unilamellar vesicles (200 nm) encapsulating a self-quenching dye. PLA_2 activity is measured by monitoring an increase in fluorescence as the dye is released from the liposomes during hydrolysis. Percent release is plotted as a function of temperature. A differential scanning calorimetry trace for DMPC unilamellar vesicles (200 nm) is also plotted showing the gel-phase regime below the pretransition at 14°C, the ripple-phase regime between the pretransition at 14°C and the main phase transition at 24°C, and the fluid-phase regime above the main phase transition at 24°C. Although the highest activity is observed in the fluid-phase regime, a clear increase in activity is observed within the ripple-phase regime compared to the gel-phase regime. The inset graph compares fluorescence traces as a function of time for large unilamellar vesicles in the gel-phase temperature regime at 8°C, and in the ripple-phase temperature regime at 18°C. The sharp initial drop in fluorescence indicates the addition of the enzyme. Fluorescence is then observed to increase immediately after addition of PLA_2 for the liposomes in the ripple-phase temperature regime, whereas the liposomes in the gel-phase temperature regime show very little increase in fluorescence in the initial stages.

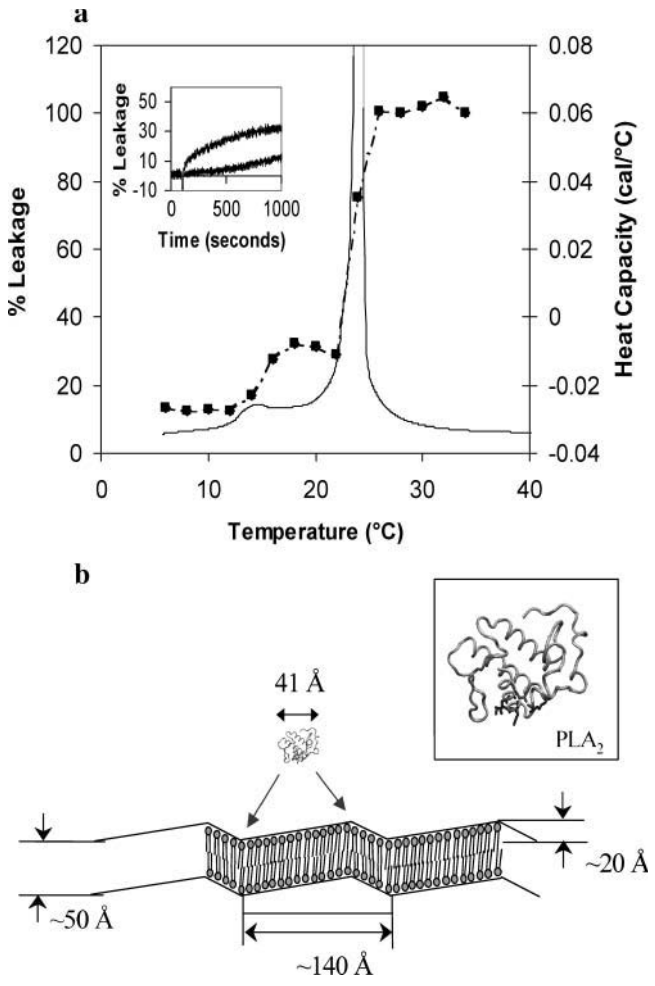

FIGURE 3 (*a*) PLA_2 hydrolysis of DMPC unilamellar vesicles (200 nm) is measured as a function of temperature by monitoring the release of a self-quenching probe (calcein) from the liposomes (■). Superimposed is a differential scanning calorimetry trace of DMPC unilamellar vesicles (200 nm) showing the pretransition at ~12°C and the main phase transition at ~24°C (*solid line*). The inset shows the time-dependent release of calcein from DMPC vesicles at 8°C (*bottom trace*) and 18°C (*upper trace*). The sharp decrease of fluorescence close to the initial time point indicates the addition of the enzyme; (*b*) comparison between the Λ/2 ripple structure with dimensions as reported by x-ray diffraction (Sun et al., 1996) drawn to scale, and the structure of snake venom PLA_2 (Han et al., 1997).

The higher susceptibility of the ripple phase to PLA_2 hydrolysis compared to the gel phase could be explained by a better accessibility of the enzyme to the lipids in the highly curved surface present in the ripple phase. The ripple structure may promote the ability of the enzyme to interact with the substrate by exposing the lipid headgroups at the high curvature regions in the ripple. Fig. 3 *b* shows a schematic illustration of the Λ/2-ripple structure for DMPC, which has been resolved by x-ray diffraction (Sun et al., 1996). The crystal structure of the snake venom PLA_2 enzyme (Han et al., 1997) is placed to scale next to the ripple structure. The illustration shows that the length scale of the ripples is relevant to the length scale of the enzyme. The illustration in Fig. 3 *b* indicates how the ripple phase can provide better access for PLA_2 hydrolysis by exposing the lipid headgroups to the catalytic pocket.

Alternatively, increased PLA_2 activity in the ripple phase could be explained by the presence of fluid-phase lipids in the ripple structure. Fluid-phase lipids show higher susceptibility toward hydrolysis than gel-phase lipids (Kaasgaard et al., 2001; Sanchez et al., 2002). A small fraction of fluid-phase lipids has been shown by x-ray diffraction to form at the pretransition temperature (Rappolt et al., 2000). Ripple formation is proposed to result from a rearrangement of this fluid-phase lipid fraction into highly ordered linear arrays, which induce the undulations in the lipid membrane (Heimburg, 2000). According to this model the ripple structure is proposed to be a band pattern of fluid- and gel-phase domains. It has been shown that PLA_2 has higher activity in the presence of coexisting fluid- and gel-phase domains (Hønger et al., 1996). The enzyme is believed to act at the interface between these domains, so the activity of PLA_2 in the ripple-phase regime could be accentuated by the presence of coexisting fluid- and gel-phase regions in the ripples. Also, a combination of both curvature effects and the presence of fluid-phase lipids at the sites of high curvature could contribute to the increased activity of PLA_2 in the

ripple-phase regime. The present study cannot distinguish between these two possibilities.

PLA_2 hydrolysis induces changes in ripple morphology while preserving bilayer integrity in a two-component DMPC/DSPC supported double bilayer

PLA_2 has very low activity toward gel phase DSPC at 24°C, resulting in a slower hydrolysis of DMPC/DSPC mixtures compared to pure DMPC bilayers (Høyrup et al., 2001a). In the following we explore how the more regulated hydrolysis of DMPC/DSPC bilayers leads to a more gradual rearrangement of the lipid membrane structure as seen through changes in ripple morphology for both the stable (Λ/2) and metastable (Λ) ripples. This is in contrast with the fast and complete degradation of the one-component DMPC double bilayer shown in Fig. 1. This slower hydrolysis also allows the lipid membrane to preserve a bilayer structure during these morphological changes.

Fig. 4 *a* shows an AFM image of the Λ/2 ripple phase forming in a 1:1 DMPC/DSPC supported double bilayer at 24°C. The ripple spacing for the DMPC/DSPC mixture is slightly larger (~200 Å) compared to the ripple spacing reported for the one-component DMPC sample (~150 Å) (Sun et al., 1996). After addition of PLA_2 to the 1:1 DMPC/DSPC sample we observe a long time period (~35 min) during which no changes in the surface are detected. As mentioned before, this period likely reflects lag time reported for bulk measurements of PLA_2 activity (Apitz-Castro et al., 1982), and is expected for DMPC/DSPC mixtures due to the lower activity of the enzyme toward DSPC (Høyrup et al., 2001a). The long lag period with no visual evidence of hydrolysis (Fig. 4 *a*) is followed by a gradual increase in the ripple spacing (Fig. 4, *b–e*) until the ripple phase finally dissipates (Fig. 4 *f*). This result is in contrast to the fast and total degradation of the lipid membrane observed for DMPC in Fig. 1.

The time evolution of the ripple profile during PLA_2 hydrolysis is shown in Fig. 4, *g–i*, corresponding to the line profiles shown in Fig. 4, *a*, *c*, and *e*. Due to the dimensions of the AFM tip (radius of curvature of sharpened tips is ~200 Å) the ripple valleys are not reached during scanning, and a noisy ripple profile is observed. Therefore, it is not possible to obtain an accurate measure for the ripple height of the Λ/2-ripple phase using this setup (Kaasgaard et al., 2003). However, the ripple spacing is accurately measured by AFM and a gradual increase in spacing during hydrolysis is clear from the results.

The increase in spacing is followed by dissipation of the ripple phase (Fig. 4 *f*). However, instead of hydrolysis resulting in complete degradation as observed for DMPC in Fig. 1 *c*, the lipid membrane continues to maintain a bilayer structure. In Fig. 5 images of the same DMPC/DSPC-

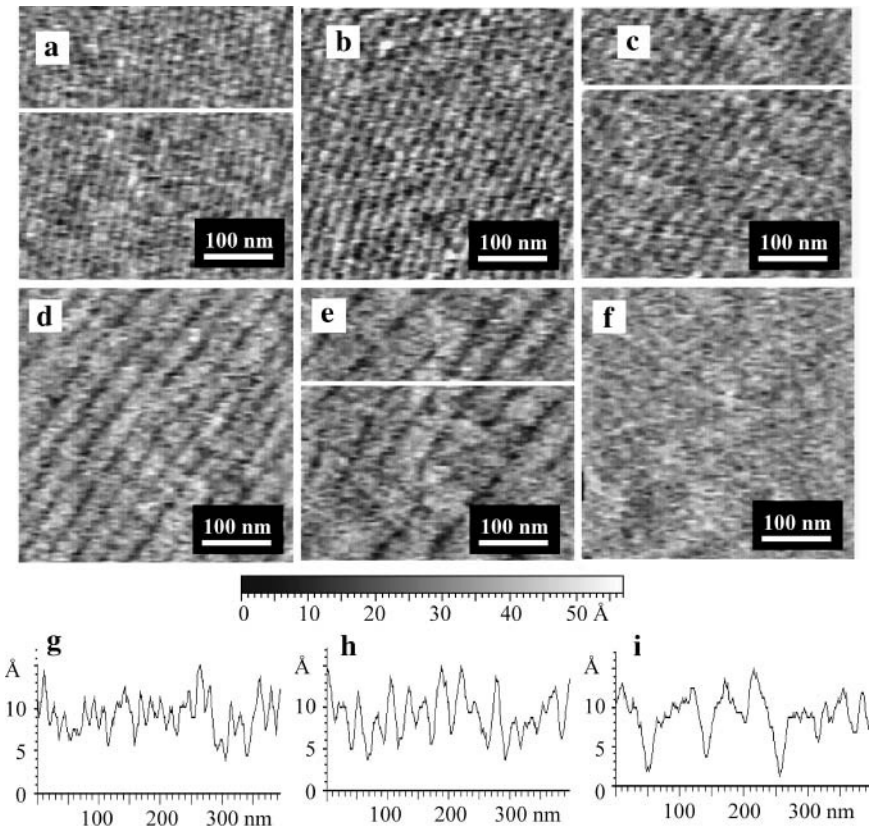

FIGURE 4 Height mode AFM images showing changes in the stable (Λ/2 spacing) ripple-phase morphology in 1:1 DMPC/DSPC supported double bilayers during PLA_2 hydrolysis. The images are taken (*a*) 29, (*b*) 42, (*c*) 44, (*d*) 46, (*e*) 50, and (*f*) 60 min after addition of PLA_2. The height profiles in *g*, *h*, and *i* correspond to the line profiles shown in images *a*, *c*, and *e*. All images are taken at 24°C.

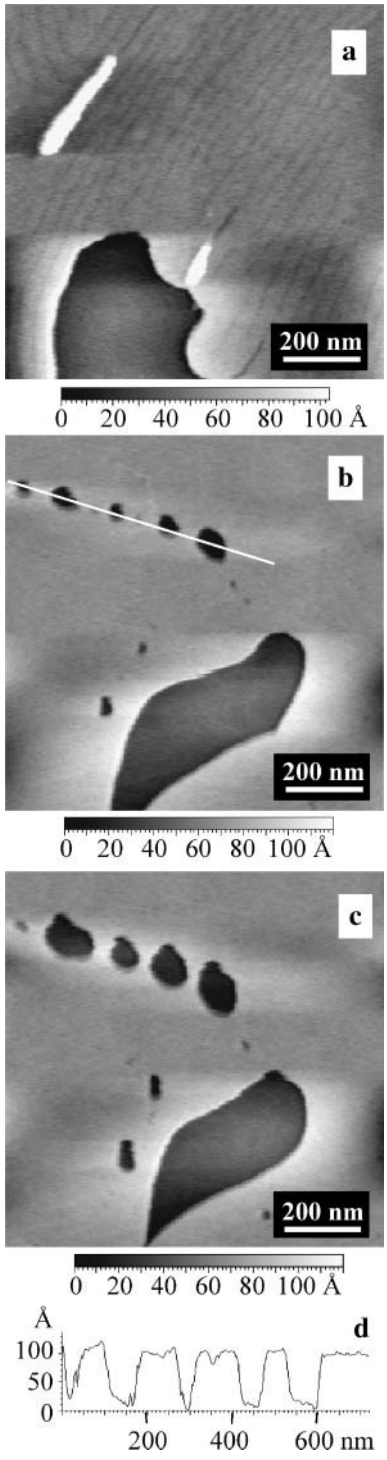

FIGURE 5 Height mode AFM images showing that the 1:1 DMPC/DSPC supported double bilayer maintains lipid membrane integrity after the ripple structure has vanished during continual hydrolysis by PLA_2. The images are at a lower magnification than those in Fig. 4, and are taken at (*a*) 46, (*b*) 60, and (*c*) 68 min after addition of PLA_2, and show the disappearance of the ripple structure (*a*), followed by formation and growth of holes in the lipid membrane as hydrolysis continues at the hole interfaces (*b* and *c*). The height profile in *d* corresponds to the white line profile in *b*, and is consistent with the expected height difference between the top and bottom supported bilayers. All images are taken at 24°C.

supported double bilayers are taken after the ripple phase has dissipated during PLA_2 hydrolysis. Fig. 5 *a* shows remnants of the ripples surrounding a large hole in the lipid membrane. This image corresponds to a zoom-out of Fig. 4 *d*. In Fig. 5 *b*, the membrane is completely flat, as the ripples have finally dissipated. The same hole as in Fig. 5 *a* appears at the bottom of the picture as reference. Fig. 5 *b* shows the formation of a series of holes in the top part of the image. These holes slowly grow with time, as would be expected for a gel-phase lipid membrane being hydrolyzed by PLA_2. The enzyme has not been inactivated so hydrolysis continues. A line profile of Fig. 5 *b* is shown in Fig. 5 *d*. The height difference is ~90 Å, corresponding to the distance between the second and the first bilayer as reported previously (Leidy et al., 2002). These results are clear indication that the membrane has undergone a structural transformation while preserving the bilayer integrity during hydrolysis.

A similar change in ripple morphology during PLA_2 hydrolysis is observed for the metastable Λ-ripple phase. Fig. 6 shows the presence of Λ-ripples in a 1:1 DMPC/DSPC supported double bilayer. The Λ-ripples have approximately double the spacing of the Λ/2 ripples (Koynova et al., 1996), making them easier to resolve by AFM, and therefore making it easier to monitor the changes in the Λ-ripple morphology during PLA_2 hydrolysis. Fig. 6, *a–d*, show a gradual increase in ripple spacing during PLA_2 hydrolysis, after a long lag phase (58 min) where no changes occur. This increase in ripple spacing is followed by a drastic collapse of the ripple structure resulting in a flat lipid membrane surface. Lipid membrane integrity is also maintained after ripple collapse (data not shown). Different ripple profiles during PLA_2 hydrolysis are shown in Fig. 6, *g–i*, corresponding to the line profiles shown in Fig. 6, *a*, *c*, and *e*. Fig. 6 *i* shows the flattened lipid membrane surface after ripple collapse.

We observe that the changes in ripple morphology during hydrolysis are similar for both Λ- and Λ/2-ripples. This behavior is plotted in Fig. 7 for both Λ- and Λ/2-ripples. In Fig. 7 *a* the increase in ripple spacing during PLA_2 hydrolysis for the Λ- and Λ/2-ripples is plotted as a function of time. A lag period is observed for both Λ- and Λ/2-ripples before any changes in ripple morphology are detected. This is in contrast to Fig. 1, where complete hydrolysis occurred almost immediately for pure DMPC ripples. The presence of longer-chained lipids has been shown to increase the lag time for hydrolysis (Høyrup et al., 2001a), which would explain the difference. The lag period is followed by a linear increase in ripple spacing for both the Λ/2- and Λ-ripples, showing very similar rates of change ~23 Å/min. The spacing is increased to 2.5 times the original spacing of the Λ/2-ripples, before the ripples cannot be detected any more, and 2.7 times the original spacing of the Λ-ripples before collapse of the ripple structure occurs (Fig. 6 *e*).

The large increase in ripple spacing suggests an expansion of the lipid membrane surface area. An accurate measurement of the increase in surface area between ripple peaks is

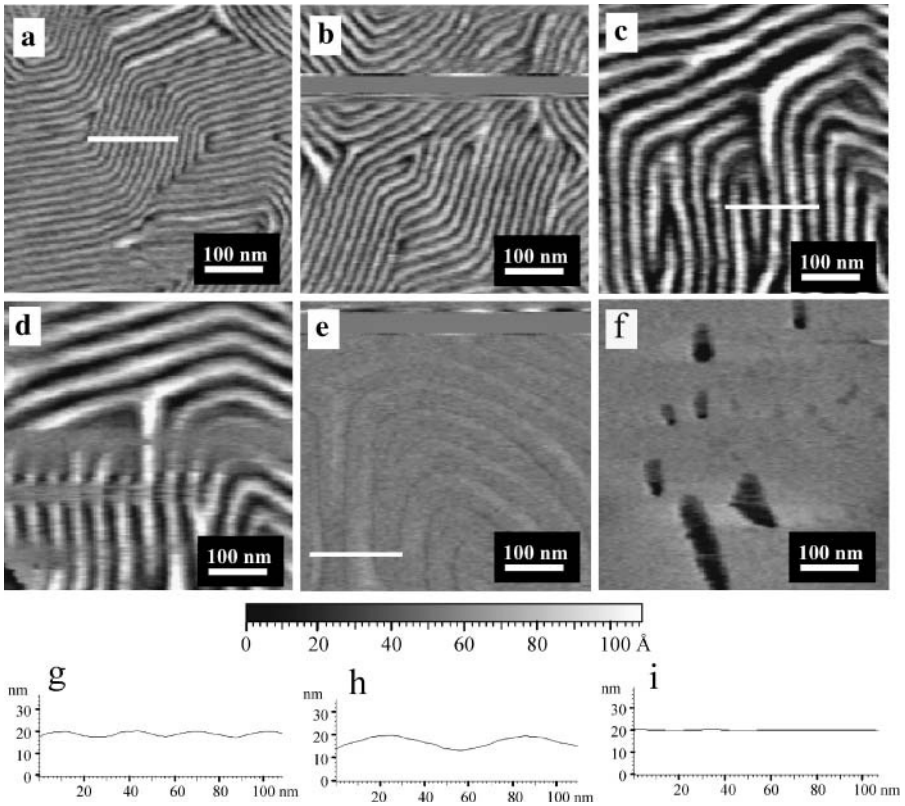

FIGURE 6 Height mode AFM images showing changes in the Λ-spacing ripple-phase morphology in 1:1 DMPC/DSPC supported double bilayers during PLA_2 hydrolysis. The images are taken (*a*) before, (*b*) 64, (*c*) 77, (*d*) 82, (*e*) 84, and (*f*) 91 min after addition of PLA_2. The height profiles in *g*, *h*, and *i* correspond to the line profiles shown in images *a*, *c*, and *e*. The height profiles are true to scale. All images are taken at 24°C.

not possible due to the tip dimensions and the tip's access to the ripple valleys. This problem is less in the case of the Λ-ripples, making it possible to monitor in a qualitative manner the ripple depth. Measurement of the ripple depth by AFM for the Λ-ripples is plotted in Fig. 7 *b* as a function of time during PLA_2 hydrolysis. The change in ripple depth is also linear, showing a drastic increase of four times the original depth.

Although the surface area cannot be measured accurately, the more than twofold increase in ripple spacing strongly suggests a large increase in lipid membrane surface area. The most likely explanation for the change in ripple morphology and increase in surface area is product accumulation, although a change in lateral membrane pressure during hydrolysis may also provide forces that undermine the ripple structure. Different additives, such as cholesterol, have been shown to increase ripple spacing (Mortensen et al., 1988). Accumulation of fatty acids and lysophospholipids, which are known to alter lipid packing (Weltzien, 1979; Senisterra et al., 1988), are likely to induce an increase in spacing as observed in Fig. 7. Since the calculated lipid concentration in the supported bilayer system is ~2 μM, lysolipid and fatty acid partitioning coefficients would suggest that most of the lysolipids and fatty acids go into solution (Høyrup et al., 2001b). However, this is a time-dependent process, which may be slow. Fig. 7 *b* also shows that after 80 min, and after reaching maximum expansion of the ripple amplitude, the lipid membrane suddenly collapses and flattens. This suggests a drastic reorganization of the lipid membrane, which could be a result of the products of hydrolysis leaving the surface. We therefore suggest that the effects of product accumulation are likely responsible for the initial changes in ripple structure, and the eventual flattening of the membrane could be a result of these products leaving the surface. PLA_2 also induces changes in the relative DMPC/DSPC composition due to preferential hydrolysis. The degree of PLA_2 hydrolysis of DMPC and DSPC in 1:1 DMPC/DSPC unilamellar vesicles (200 nm) in the ripple-phase regime (24°C) was measured by HPLC chromatography as a function of time (data not shown). The results show that DMPC is preferentially hydrolyzed by PLA_2 at this temperature. After 20 min, 80% of the DMPC in the sample was hydrolyzed, whereas DSPC showed no measurable degree of hydrolysis. Since hydrolysis products are expected to eventually leave the surface, the change in relative composition will be the dominating factor in the final state of the supported bilayer. The change in composition induced by PLA_2 explains the conversion from a ripple-phase lipid membrane to a gel-phase lipid membrane. DSPC has a high main phase transition ~55°C and a high pretransition ~52°C. A gradual enrichment of DSPC during hydrolysis will drive the lipid membrane from a ripple-phase regime into a gel-phase regime. In addition, the transition toward a DSPC-enriched composition resulting in a gel-phase lipid membrane reduces the susceptibility of the lipid membrane toward further PLA_2 hydrolysis (Høyrup et al., 2001a).

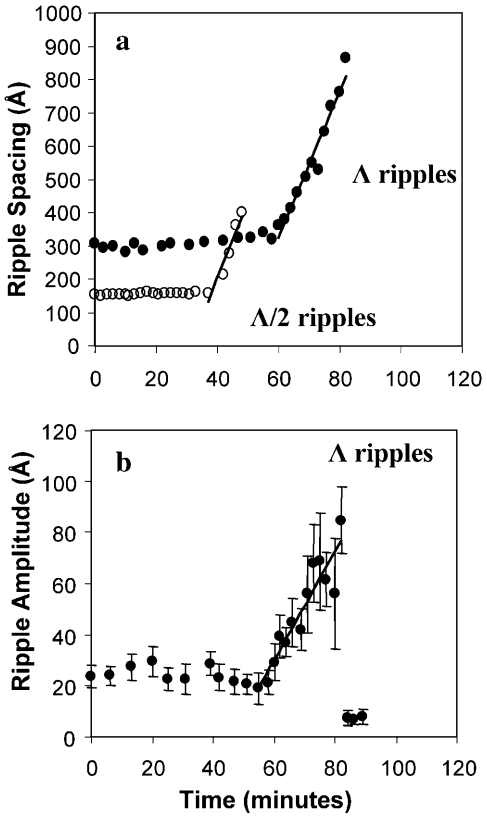

FIGURE 7 (*a*) Changes in ripple spacing as a function of time after addition of PLA_2 for the stable (○) and metastable (●) ripple phase as measured by Fourier transform; (*b*) changes in ripple amplitude as a function of time after addition of PLA_2 for the metastable ripple phase as measured by averaging height profiles of more than 20 ripples. The change in ripple amplitude for the stable ripple phase is not reported due to the low resolution caused by reduced access of the AFM tip into the ripple valleys.

Preferential hydrolysis of PLA_2 along the ripple direction in both Λ/2 and Λ-ripples in a two-component DMPC/DSPC supported double bilayer

Fig. 8 shows that holes formed by PLA_2 hydrolysis preferentially form along the direction of the ripple structure. Fig. 8 *a* shows the presence of Λ/2-ripples in a 1:1 DMPC/DSPC supported double bilayer as the lipid membrane is hydrolyzed by PLA_2. The holes that are forming during hydrolysis stretch parallel to the ripple direction. Fig. 8 *b* shows the Λ-ripple phase in a 1:1 DMPC/DSPC supported double bilayer, during continual PLA_2 hydrolysis, showing that after collapse a hole has formed in parallel to the direction of the ripples. Fig. 8 *c* shows another example where holes form in parallel to the Λ-ripple phase after the collapse of the ripple structure. The hydrolysis along the ripple direction appears to occur within the ripple valleys (Fig. 8, *a* and *b*), indicating that the high curvature regions are susceptible to hydrolysis. It is intriguing that the formation of holes occurs only at the valleys, and not at the cusps. As indicated in Fig. 3 *b* we suggest that both the ripple cusps and the ripple valleys could show higher susceptibility to hydrolysis. Since the holes are formed at the valleys, it appears that the valley regions are most sensitive to hydrolysis. What is clear from the results is that hole formation occurs along the direction of the ripples, indicating the presence of anisotropic regions (strips) within the ripple structure that show a higher susceptibility to hydrolysis.

CONCLUSION

The results presented in this paper show increased activity of PLA_2 toward the ripple phase compared to the gel phase. This appears to reflect a higher sensitivity of PLA_2 toward curved lipid membrane surfaces, and partly disordered lipids. Fig. 3 *b* illustrates that the ripple dimensions would be expected to influence PLA_2 activity, supporting the notion that the ripple structure provides higher accessibility for the enzyme to the substrate, in particular at the ripple cusps. The higher sensitivity could also be a result of the presence of fluid-phase lipids as suggested in the model by Heimburg (2000), which proposes that the ripples are a result of a nano-structural array of fluid-phase and gel-phase lipids. Fig. 8 shows evidence that holes resulting from hydrolysis form along the ripple direction. The formation of anisotropic holes implies that the ripple structure has regions or strips, running parallel to the ripple direction, that show higher sensitivity to hydrolysis. These holes appear for both Λ- and Λ/2- ripples,

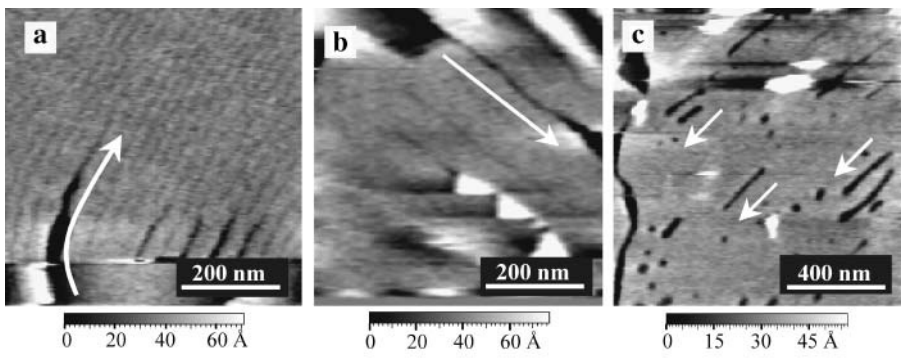

FIGURE 8 Evidence for PLA_2 hydrolysis at the ripple valleys. Hole formation along the ripple direction induced by PLA_2 hydrolysis is observed in 1:1 DMPC/DSPC supported double bilayers. (*a*) Hydrolysis takes place along the ripple direction for the stable ripple phase; (*b*) metastable ripples also show evidence of hydrolysis along the ripple direction, which appear as elongated holes after the lipid membrane flattens during PLA_2 hydrolysis; and (*c*) hydrolysis of metastable ripples in the fluid-ripple coexistence regime also shows evidence of hydrolysis along the ripple direction with the appearance of elongated holes after flattening. All arrows run in parallel to the holes.

making it a general characteristic of the ripple structure. We suggest that these strips that are more sensitive to degradation could be characterized by having either high curvature or fluid-phase lipids. On the other hand, the strip regions that are not hydrolyzed could be resistant due to a high degree of hexagonal headgroup packing, and a decreased access to the ester linkage in the *sn*-2 position.

In the DMPC/DSPC mixtures hydrolysis is slower, so instead of complete hydrolysis of the lipid membrane we observe a gradual change in lipid membrane morphology that occurs while preserving lipid membrane integrity. In both Λ- and Λ/2-ripple structures an increase in ripple spacing is followed by the collapse of the ripples and the formation of a gel-phase lipid membrane. HPLC results show that DMPC is preferentially hydrolyzed within the ripple-phase temperature regime. DSPC has a main phase transition at ~55°C and a pretransition at ~52°C, so enrichment in DSPC explains the transformation of the lipid membrane into gel phase. These results provide direct evidence, within a model system, of morphological changes in the lipid membrane induced by PLA_2 activity. It is shown that PLA_2 activity can be regulated by composition, and that the more gradual hydrolysis observed in the DMPC/DSPC system results in changes in lipid membrane morphology through gradual changes in lipid membrane composition. It is also important to note that these morphological changes occur whereas the lipid membrane still maintains a bilayer structure, which points to the usefulness of PLA_2 as a remodeling tool for the lipid membrane. A combination of preferential hydrolysis and the right enzyme kinetics leads to changes in the lipid membrane phase state and the lipid membrane morphology.

In general, these results are clear evidence that PLA_2 can induce a compositional phase transition in a lipid membrane through preferential hydrolysis while still preserving lipid membrane integrity. At the cellular level, PLA_2 has been implicated in inducing morphological changes in the lipid membrane during cell membrane remodeling (Brown et al., 2003; Geddis and Rehder, 2003). However, the focus of PLA_2 activity has been on its role as a generator of signaling molecules, inducing these changes in an indirect manner (Murakami and Kudo, 2002). The current results show that preferential hydrolysis may be a mechanism by which PLA_2 can induce changes in membrane morphology and phase state directly, independent of the generation of signaling molecules.

The authors thank Thomas Kaasgaard for helpful discussions.

MEMPHYS-Center for Biomembrane Physics is supported by the Danish National Research Foundation.

REFERENCES

Apitz-Castro, R., M. K. Jain, and G. H. De Haas. 1982. Origin of the latency phase during the action of phospholipase A_2 on unmodified phophatildylcholine vesicles. *Biochim. Biophys. Acta.* 688:349–356.

Bell, J. D., and R. L. Biltonen. 1989. Thermodynamic and kinetic studies of the interaction of vesicular dipalmytoylphosphatidylcholine with *agkistrodon-piscivorus-piscivorus* phospholipase A_2. *J. Biol. Chem.* 264:225–230.

Brown, W. J., K. Chambers, and A. Doody. 2003. Phospholipase A_2 (PLA_2) enzymes in membrane trafficking: Mediators of membrane shape and function. *Traffic.* 4:214–221.

Burack, W. R., and R. L. Biltonen. 1994. Lipid bilayer heterogeneities and modulation of phospholipase A_2 activity. *Chem. Phys. Lipids.* 73: 209–222.

Burack, W. R., A. R. G. Dibble, M. M. Allietta, and R. L. Biltonen. 1997a. Changes in vesicle morphology induced by lateral phase separation modulate phospholipase A_2 activity. *Biochemistry.* 36:10551–10557.

Burack, W. R., A. R. G. Dibble, and R. L. Biltonen. 1997b. The relationship between compositional phase separation and vesicle morphology: Implications for the regulation of phospholipase A_2 by membrane structure. *Chem. Phys. Lipids.* 90:87–95.

Burack, W. R., Q. Yuan, and R. L. Biltonen. 1993. Role of lateral phase-separation in the modulation of phospholipase-A_2 activity. *Biochemistry.* 32:583–589.

Dennis, E. A., P. L. Darke, R. A. Deems, C. R. KensilL, and A. Pluckthun., 1981. Cobra venom phospholipase-A_2. A review of its action towards lipid-water interfaces. *Mol. Cell. Biochem.* 36:37–45.

Doniach, S. 1979. A thermodynamic model for the monoclinic (ripple) phase of hydrated phospholipid bilayers. *J. Chem. Phys.* 70:4587–4596.

Fernandez, M. S., R. Mejia, and E. Zavala. 1991. The interfacial calcium-ion concentration as a modulator of the latency phase in the hydrolysis of dimyristoylphosphatidylcholine liposomes by phospholipase A_2. *Biochem. Cell. Biol.* 69:722–727.

Fragneto, G., T. Charitat, F. Graner, K. Mecke, L. Perino-Gallice, and E. Bellet-Amalric. 2001. A fluid floating bilayer. *Europhys. Lett.* 53: 100–106.

Geddis, M. S., and V. Rehder. 2003. Initial stages of neural regeneration in *Helisoma trivolvis* are dependent upon PLA_2 activity. *J. Neurobiol.* 54:555–565.

Giocondi, M. C., L. Pacheco, P. E. Milhiet, and C. Le Grimellec. 2001. Temperature dependence of the topology of supported dimirystoyl-distearoyl phosphatidylcholine bilayers. *Ultramicroscopy.* 86:151–157.

Grandbois, M., H. Clausen-Schaumann, and H. Gaub. 1998. Atomic force microscope imaging of phospholipid bilayer degradation by phospholipase A_2. *Biophys. J.* 74:2398–2404.

Han, S. K., E. T. Yoon, D. L. Scott, P. B. Sigler, and W. Cho. 1997. Structural aspects of interfacial adsorption. A crystallographic and site-directed mutagenesis study of the phospholipase A_2 from the snake venom of Agkistrodon piscivorus piscivorus. *J. Biol. Chem.* 227:3573–3582.

Heimburg, T. 2000. A model for the lipid pretransition: coupling of ripple formation with the chain-melting transition. *Biophys. J.* 78:1154–1165.

Henshaw, J. B., C. A. Olsen, A. R. Farnbach, K. H. Nielson, and J. D. Bell. 1998. Definition of the specific roles of lysolecithin and palmitic acid in altering the susceptibility of dipalmitoylphosphatidylcholine bilayers to phospholipase A_2. *Biochemistry.* 37:10709–10721.

Hønger, T., K. Jørgensen, R. L. Biltonen, and O. G. Mouritsen. 1996. Systematic relationship between phospholipase A_2 activity and dynamic lipid bilayer microheterogeneity. *Biochemistry.* 35:9003–9006.

Høyrup, P., J. Davidsen, and K. Jørgensen. 2001b. Lipid membrane partitioning of lysolipid and fatty acids: Effects of membrane phase structure and detergent chain length. *J. Phys. Chem. B.* 105:2649–2657.

Høyrup, P., K. Jørgensen, and O. G. Mouritsen. 2002. Phospholipase A_2 — An enzyme that is sensitive to the physics of its substrate. *Europhys. Lett.* 57:464–470.

Høyrup, P., O. G. Mouritsen, and K. Jørgensen. 2001a. Phospholipase A_2 activity towards vesicles of DPPC and DMPC-DSPC containing small amounts of SMPC. *Biochim. Biophys. Acta.* 1515:133–143.

Kaasgaard, T., J. H. Ipsen, O. G. Mouritsen, and K. Jørgensen. 2001. In situ phospholipase A_2 degradation of one- and two-component phospholipid

bilayers imaged by atomic force microscopy. *Probe Microscopy*. 2: 169–175.

Kaasgaard, T., C. Leidy, J. H. Crowe, O. G. Mouritsen, and K. Jørgensen. 2003. Temperature-controlled structure and kinetics of ripple phases in one- and two-component supported lipid bilayers. *Biophys. J*. 85: 350–360.

Katsaras, J., S. Tristram-Nagle, Y. Liu, R. L. Headrick, E. Fontes, P. C. Mason, and J. F. Nagle. 2000. Clarification of the ripple phase of lecithin bilayers using fully hydrated, aligned samples. *Phys. Rev. E*. 61:5668–5677.

Kensil, C. R., and E. A. Dennis. 1979. Action of cobra venom phospholipase-A_2 on the gel and liquid-crystalline states of dimyristoyl and dipalmitoyl phosphatidylcholine vesicles. *J. Biol. Chem*. 254:5843–5848.

Koynova, R., A. Koumanov, and B. Tenchov. 1996. Metastable rippled gel phase in saturated phosphatidylcholines: calorimetric and densitometric characterization. *Biochim. Biophys. Acta*. 1285:101–108.

Leidy, C., T. Kaasgaard, J. H. Crowe, O. G. Mouritsen, and K. Jørgensen. 2002. Ripples and the formation of anisotropic lipid domains: imaging two-component supported double bilayers by atomic force microscopy. *Biophys. J*. 83:2625–2633.

Lubensky, T. C., and F. C. Mackintosh. 1993. Theory of the ripple phases of lipid bilayers. *Phys. Rev. Lett*. 71:1565–1568.

Mao-Qiang, M., K. R. Feingold, M. Jain, and P. M. Elias. 1995. Extracellular processing of phospholipids is required for permeability barrier homeostasis. *J. Lipid Res*. 36:1925–1935.

Mortensen, K., W. Pfeiffer, E. Sackmann, and W. Knoll. 1988. Structural properties of a phosphatidylcholine-cholesterol system as studied by small-angle neutron scattering: ripple structure and phase diagram. *Biochim. Biophys. Acta*. 945:221–245.

Murakami, M., and I. Kudo. 2002. Phospholipase A_2. *J. Biochem*. 131: 285–292.

Nagle, J. F., and S. Tristram-Nagle. 2000. Structure of lipid bilayers. *Biochim. Biophys. Acta*. 1469:159–195.

Nevalainen, T. J., M. M. Haapamaki, and J. M. Gronroos. 2000. Roles of secretory phospholipases A_2 in inflammatory diseases and trauma. *Biochim. Biophys. Acta*. 1488:83–90.

Nielsen, L. K., J. Risbo, T. H. Callisen, and T. Bjørnholm. 1999. Lag-burst kinetics in phospholipase A_2 hydrolysis of DPPC bilayers visualized by atomic force microscopy. *Biochim. Biophys. Acta*. 1420:266–271.

Peters, G. H., U. Dahmen-Levison, K. de Meijere, G. Brezesinski, S. Toxvaerd, H. Möhwald, A. Svendsen, and P. K. J. Kinnunen. 2000. Influence of surface properties of mixed monolayers on lipolytic hydrolysis. *Langmuir*. 16:2779–2788.

Rappolt, M., G. Pabst, G. Rapp, M. Kriechbaum, H. Amenitsch, C. Krenn, S. Bernstorff, and P. Laggner. 2000. New evidence for gel-liquid crystalline phase coexistence in the ripple phase of phosphatidylcholines. *Eur. Biophys. J*. 29:125–133.

Sanchez, S. A., L. A. Bagatolli, E. Gratton, and T. L. Hazlett. 2002. A two-photon view of an enzyme at work: Crotalus atrox venom PLA2 interaction with single-lipid and mixed-lipid giant unilamellar vesicles. *Biophys. J*. 82:2232–2243.

Senisterra, G. A., E. A. Disalvo, and J. J. Gagliardino. 1988. Osmotic dependence of the lysophosphatidylcholine lytic action on liposomes in the gel state. *Biochim. Biophys. Acta*. 941:264–270.

Six, D. A., and E. A. Dennis. 2000. The expanding superfamily of phospholipase A_2 enzymes: classification and characterization. *Biochim. Biophys. Acta*. 1488:1–19.

Sun, W.-J., S. Tristram-Nagle, R. M. Suter, and J. F. Nagle. 1996. Structure of the ripple phase in lecithinábilayers. *Proc. Natl. Acad. Sci. USA*. 93:7008–7012.

Tenchov, B. G., H. Yao, and I. Hatta. 1989. Time-resolved x-ray diffraction and calorimetric studies at low scan rates. I. Fully hydrated dipalmitoyl-phosphatidylcholine (DPPC) and DPPC/water/ethanol phases. *Biophys. J*. 56:757–768.

Verger, R., M. C. E. Mieras, and G. H. de Haas. 1973. Action of phospholipase a2 at interfaces. *J. Biol. Chem*. 248:4023–4034.

Waite, M. 1991. Phospholipases. *In* Biochemistry of Lipids, Lipoptoteins and Membranes. D. E. Vance and J. Vance, editors. Elsevier Science Publishers B. V., Amsterdam, The Netherlands. 269–295.

Weltzien, H. U. 1979. Cytolytic and membrane-perturbing properties of lysophosphatidylcholine. *Biochim. Biophys. Acta*. 559:259–287.

Zasadzinski, J. A., J. Schneir, J. Gurley, V. Elings, and P. K. Hansma. 1988. Scanning tunneling microscopy of freeze-fracture replicas of biomembranes. *Science*. 239:1013–1015.